Toward true closed-loop neuromodulation: artifact-free recording during stimulation

Andy Zhou[1], Benjamin C Johnson[1] and Rikky Muller

Closed-loop and responsive neuromodulation systems improve open-loop neurostimulation by responding directly to measured neural activity and providing adaptive, on-demand therapy. To be effective, these systems must be able to simultaneously record and stimulate neural activity, a task made difficult by persistent stimulation artifacts that distort and obscure underlying biomarkers. To enable simultaneous stimulation and recording, several techniques have been proposed. These techniques involve artifact-preventing system configurations, resilient recording front-ends, and back-end signal processing for removing recorded artifacts. Co-designing and integrating these artifact cancellation techniques will be key to enabling neuromodulation systems to stimulate and record at the same time. Here, we review the state-of-the-art for these techniques and their role in achieving artifact-free neuromodulation.

Address
Department of Electrical Engineering and Computer Sciences, University of California, Berkeley, 2108 Allston Way, Suite 200, Berkeley, CA 94704, United States

Corresponding author: Muller, Rikky (rikky@berkeley.edu)
[1] Equally contributing first authors.

Introduction

The past decade has seen a surge of clinical applications for neural recording and stimulation in the treatment of neurological disorders. For instance, responsive neurostimulation for treating epilepsy uses recorded neural biomarkers to trigger therapeutic stimulation [1–3]. Deep brain stimulation (DBS) is another therapy widely researched and clinically prescribed for the treatment of Parkinson's disease [4,5]. Closed-loop DBS has recently been proposed to only deliver stimulation when the patient is symptomatic, improving battery life and reducing side effects [6–8]. Looking forward, closed-loop therapies can be utilized to treat complex conditions whose symptoms are not always present, necessitating simultaneous sensing, biomarker computation, and targeted therapeutic stimulation in the brain.

Today, there are major limitations in using therapeutic stimulation in a closed-loop, on-demand manner. Stimulation pulses create interference with recording electronics, which appear as artifacts masking the underlying neural signal and making simultaneous sensing and stimulating a challenge [9]. To record continuous neural activity while simultaneously delivering stimulation, neuromodulation systems must be resistant to large stimulation artifacts and be able to actively remove artifacts from the digitized signals for real-time biomarker computation (Figure 1). Here we review artifact mitigation techniques: artifact prevention, resilient recording front-ends for improved artifact immunity, and back-end digital signal processing for artifact removal. We conclude that system integration of multiple techniques produces the best results for enabling closed-loop artifact-free neuromodulation.

Origin and prevention of stimulation artifacts

Stimulation artifacts typically consist of large voltage transients coinciding with the delivery of stimulation pulses. Their morphologies are dependent upon stimulator architecture and performance, stimulation waveform, and electrode configuration. Recorded artifacts consist of a short, high-amplitude peak (direct artifact) followed by a slow, exponential decay (residual artifact) superimposed on the local neural activity. Cancellation of these artifact components is crucial for analyzing spikes, as well as local field potentials (LFP) and electrocorticography (ECoG). Artifacts may be misclassified as spikes by some detection algorithms, and subsequent spikes cannot be recorded until the electrode voltage has returned to within the input range of the recording amplifier. The artifact peaks and ensuing decay together create strong distortions in the power spectrum at the stimulation frequency and also spreading into frequency bands of interest for LFP and ECoG.

To demonstrate the origin of stimulation artifacts, a simplified electrical model of an electrode with biphasic current stimulation is shown in Figure 2. The electrode double-layer capacitance (C_{DL}), charge-transfer resistance (R_{CT}), and spread resistance (R_S) are primarily functions of an electrode's area, geometry, surface roughness, and material [10]. Artifacts arise from voltage drops across stimulating electrodes and tissue as current passes

Figure 1
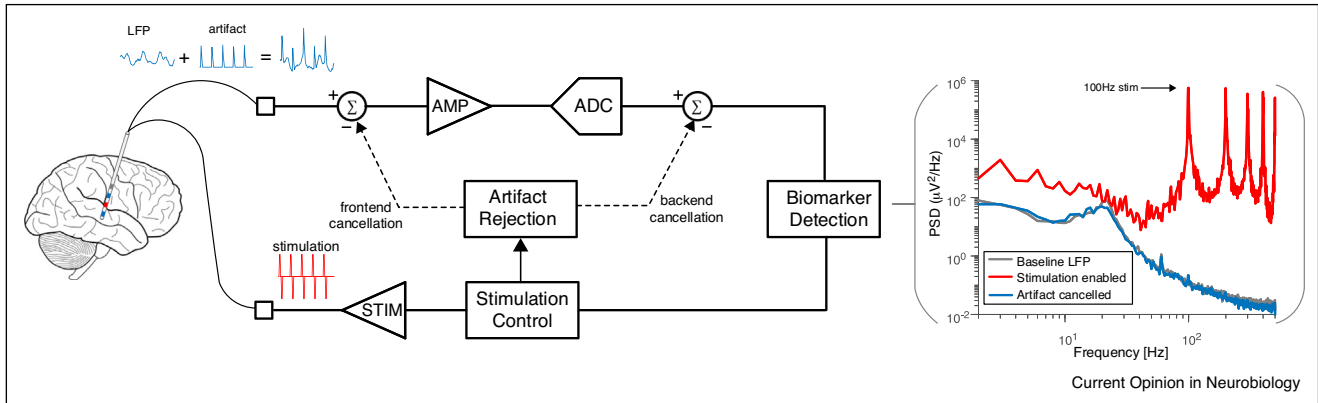
An example of adaptive closed-loop neuromodulation using local field potential feedback. Stimulation artifacts contaminate the recorded signal and prevent robust detection of biomarkers. Note that even an out-of-band stimulation signal can corrupt the entire sensing spectrum. To enable real-time feedback, neuromodulation systems attempt to mitigate artifact through the electrode configuration, resilient recording front-ends, and back-end cancellation methods.

Figure 2
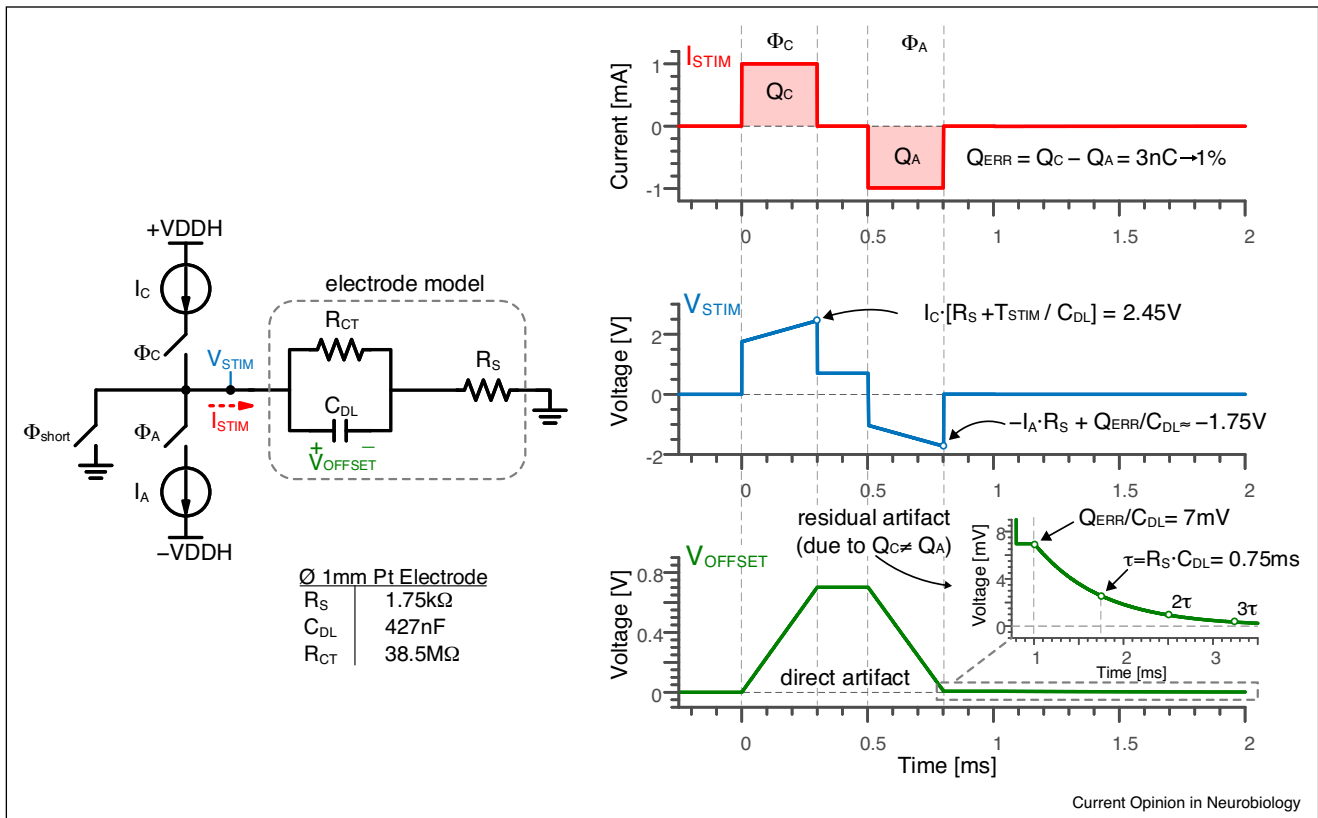
Electrical model of the stimulation electrode and resulting current and voltage waveforms. Stimulation artifact, V_{OFFSET}, is a function of the stimulation current and electrode. Residual artifact duration, shown in the inset of V_{OFFSET}, depends on the accuracy of the charge balance and the time constant associated with dissipating residual charge stored on C_{DL}. Any mismatch in the stimulation phases (e.g. between I_C and I_A) means charge will remain on the capacitors, resulting in a voltage of Q_{ERR}/C_{DL}. This residual charge will leak away slowly ($\tau \sim R_S C_{DL}$). Front-ends must accommodate the large transient portion of the artifact and the slow discharge.

through them. This artifact will also propagate through the spread resistance to all of the other recording electrodes in the array. Precise modeling of the artifact is difficult since electrode impedance is nonlinear and varies with voltage. Furthermore, electrode impedance can change over time with chronic implantation [11]. The linear model, however, is effective for estimating the peak voltage due to stimulation and duration of an artifact [12•,13,14].

Ideally, the cathodic and anodic phases of biphasic stimulation are perfectly matched with the same amount of charge ($Q_C = Q_A$) and completely discharge the electrode capacitance, C_{DL}. In this case, the system would only experience direct artifact. However, any mismatch in current amplitude ($I_C \neq I_A$) or pulse width ($\Phi_C \neq \Phi_A$) leaves residual charge on the capacitors, resulting in DC voltage offset, a persisting artifact voltage that discharges slowly (Figure 2, residual artifact on V_{OFFSET}). Residual artifact duration depends on the degree of mismatch and the time constant associated with dissipating residual charge. Aside from saturating recording front-ends, slow discharge can limit stimulation frequency since accumulated charge creates a DC current at the electrode, resulting in tissue damage and corrosion from electrolysis [10,15].

Several techniques have been utilized to improve stimulator phase matching. Pulse timing is typically well-controlled, whereas different current sources commonly have an amplitude mismatch of 1%, which is enough to produce significant artifact [12•]. Some systems monitor V_{OFFSET} at the electrode from accumulated charge and calibrate the second phase current to minimize this offset [16]. Other systems calibrate prior to stimulation via current-copying using the using the cathodic current source as a reference for the anodic current [17,18]. Another alternative uses an H-bridge circuit, which is a stimulator topology that utilizes a single current source and a set of switches that allows the same current source to be used in both stimulation phases [19••,20,21]. This method has been shown to achieve a mismatch between pulses of less than 0.02% [19••].

Even stimulation pulses that are perfectly balanced with equal charge in each phase can generate large and long artifacts if recorded using inadequate circuits. Some work uses a tri-phasic stimulation waveform to minimize artifact duration [22]. Chu et al. [23] took an alternative approach by modeling the brain and interface as a communication channel and designing a waveform shape that inverts the transfer function, thereby reducing the artifact duration by 73%.

Deliberate placement of stimulation, recording, and reference electrodes has also been shown to reduce the stimulation artifact. For example, a symmetric configuration between stimulation and recording electrodes can present the artifact as a common-mode signal, which can more easily be rejected by differential recording amplifiers [24••]. Peterson et al. [25] eliminated a common ground between the recording and stimulation subsystems, allowing the recording reference to track common-mode artifacts. So far, the presented prevention techniques do not entirely eliminate artifacts, but do ease requirements on front-end acquisition.

Design for front-end artifact immunity

High fidelity recording of extracellular neural activity requires low-noise instrumentation to detect neural signals down to microvolt amplitudes. Noise performance trades off with power consumption, so recording front-ends, consisting of neural signal amplification and digitization circuitry, typically dominate the overall power of a neural recording system [26,27]. As a result, neural recording designs have primarily focused on optimizing power efficiency to extend battery life, reduce wireless power harvesting requirements, or minimize heat dissipation [28–31]. As recording systems scale to higher channel counts (>1000), power-efficient design is further exacerbated by tight area constraints [32–34] and high communication data rates [35].

Due to these constraints, most existing neural recording designs have not considered concurrent stimulation and are susceptible to artifacts. For example, power-efficient front-ends typically have a large gain to maximize their sensitivity. A high gain reduces the power requirements of subsequent processing stages, such as an analog-to-digital converter (ADC), but also causes the amplifier to saturate when presented with large stimulation artifacts. Furthermore, conventional front-ends utilize a low frequency high-pass corner to block DC offsets [29–31], but this results in a slow recovery from saturation due to the large, rapid transient voltage of a stimulation artifact (Figure 3a).

Newer front-end techniques have focused on mitigating the effects of stimulation artifacts by preventing saturation. One such technique is to increase the dynamic range of the recording circuits, enabling them to withstand and record larger voltages without significantly increasing the electronic noise (Figure 3b). A direct approach is to lower the amount of signal amplification [36]. A smaller artifact can remain in the linear range of the amplifier, so signal linearity is maintained and stimulation artifact can, in theory, be removed digitally in the back-end. However, this method sacrifices power efficiency by necessitating a higher supply voltage and a higher-resolution ADC for signal digitization. Another approach is to reduce the requirement for a large dynamic range by subtracting, using hardware methods, a model of the artifact at the input during stimulation to keep signals within a smaller range (Figure 3f). The model of the artifact is learned

Figure 3
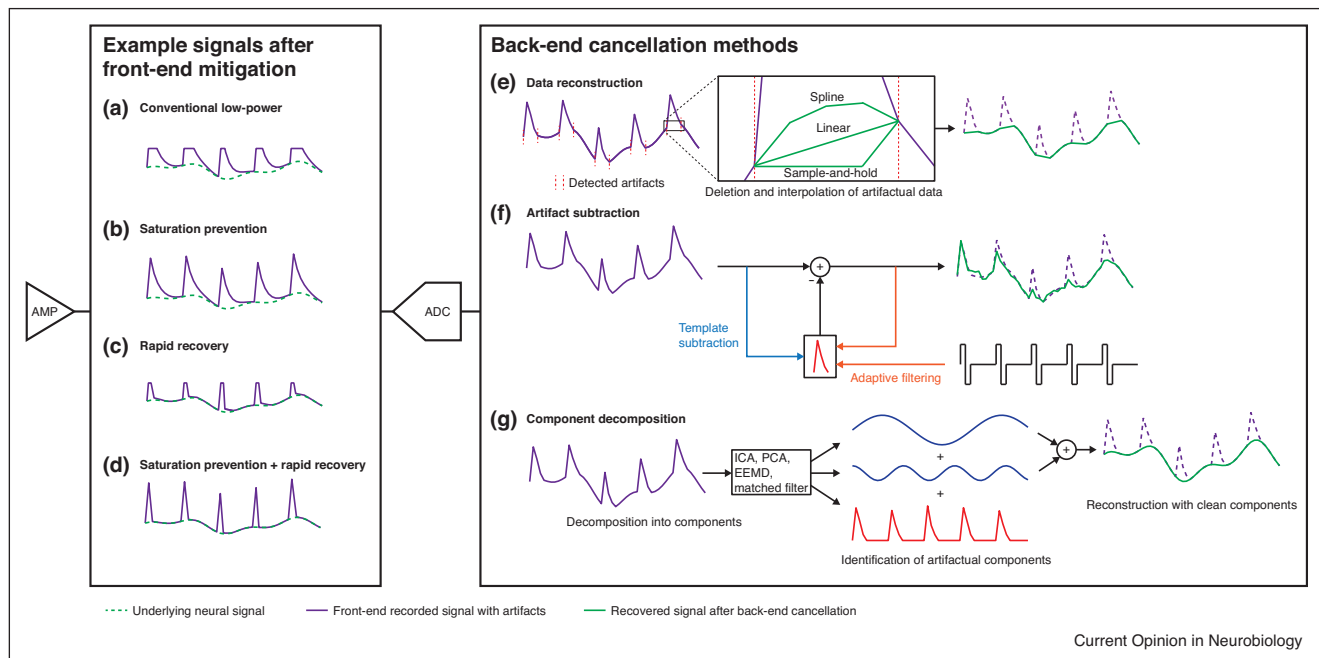
Front-end artifact mitigation techniques improve linearity and duration of recorded artifacts, and back-end methods remove them. Examples of signals recorded by front-ends utilizing different mitigation methods are shown (left), followed by descriptions of back-end cancellation methods (right). Recorded analog signals (solid purple) contain artifacts that distort the underlying neural signal (dotted green) to various degrees. Back-end cancellation methods attempt to recover the neural signal (solid green). **(a)** With typical recording front-ends, artifacts saturate the amplifier and the amplifier recovers slowly. **(b)** Saturation can be prevented by increasing the dynamic range of the front-end, lowering signal distortion and enabling subtractive back-end methods. **(c)** By contrast, front-ends that quickly recover from a saturating signal can minimize the amount of distorted data. **(d)** Ideal systems implement both saturation prevention and rapid recovery, resulting in simple-to-cancel artifacts. **(e)** Simplest back-end techniques identify the artifact segments and reconstruct the underlying data using interpolation. **(f)** Subtractive methods remove artifact by subtracting estimated artifact waveforms. Estimation is done through template building or adaptive filtering. **(g)** Recorded waveforms can be separated into artifactual and neural components. Clean neural components are used to reconstruct the underlying signal.

through template building [32,37], filtering the stimulation pulse [38•], or creating a replica artifact signal [39]. This technique holds promise, but can degrade the signal-to-noise ratio (SNR) of the underlying neural signal [38•]. Alternatively, disconnecting the front-end via a series switch at the input prevents artifacts from reaching the recording circuitry [1,40–43]. However, this approach can suffer from slow transient settling once reconnected.

While spikes may be detected and analyzed even when superimposed on the long decays following amplifier saturation, these settling responses severely degrade LFP and ECoG signals. Thus, a resilient recording front-end must also rapidly recover from a saturating signal (Figure 3c). Resetting the recording circuits at every sample can clear the saturating charge and eliminate the long transient responses that result. Several designs add hard reset switches [19••,44] or a controllable weak resistance [12•,45,46] to reset the amplifier and rapidly return to the baseline voltage. In some cases, stimulation causes charge to accumulate on the recording electrode, so some work actively discharges the electrode itself to an averaged pre-stimulus voltage [12•,13,14].

Johnson *et al.* [19••] combines techniques by resetting at every sample while also increasing front-end dynamic range (Figure 3d). The design uses a mixed-signal approach that combines analog and digital domains, and places the ADC inside the amplifier feedback loop. This has several advantages, as it reduces normally saturating signal swings while providing the same overall gain, allowing for an increased input range of 100 s of mV while maintaining power and noise performance.

Back-end neural signal recovery
Back-end signal processing techniques can be applied to the digitized signals at the ADC output to remove remaining stimulation artifacts. We divide these techniques into three categories: firstly, data reconstruction (Figure 3e), secondly, artifact subtraction (Figure 3f), and thirdly, component decomposition (Figure 3g). Although many of these techniques originated as offline methods, some have been implemented online for real-time artifact cancellation. Closed-loop and responsive applications require fast, low-complexity, and low-power online implementations.

Reconstruction methods remove samples contaminated with artifacts and replace them with interpolated values (Figure 3e). Sample-and-hold methods hold over the last known good sample for the duration of each artifact [47,48]. This requires only a single sample of memory, but may cause significant distortion. To reduce distortion, samples may be replaced by linear interpolation between the nearest clean samples [49•,50•], an estimation from a learned Gaussian probability density for data segments [51], or a reconstruction using cubic spline interpolation [52]. Hoffman *et al*. [51] report an SNR of between 30 and 40 dB for linear interpolation and Gaussian estimation, and Zhou *et al*. [49•] show that baseline power spectral density for LFP could be accurately recovered after linear interpolation over artifacts.

Although simple to implement, data reconstruction requires artifact detection. This can be done using blind detection algorithms [48,50•,51], or using timing indicators from the stimulator [19••,37,49•]. These methods lose information during the artifact, degrading SNR and potentially also removing action potentials which are typically shorter in duration than the artifact. Thus, interpolation is better suited to lower frequency recordings like LFP and ECoG than spike recordings. Ideally, this technique is paired with rapid recovery front-ends to keep the artifact short. High dynamic range is less critical as saturated data is discarded anyway.

High dynamic range front-ends, however, are essential for subtraction and component decomposition techniques, which require the undistorted artifact waveform. These algorithms assume that the artifact is linearly superimposed onto the neural signal and can be subtracted either sample-by-sample or as an interference source. Theoretically, decomposition and subtraction allow for the most accurate recovery of the underlying signal, crucial for spike detection and sorting.

First introduced as an offline method [48,53,54], template subtraction has been implemented in both online hardware [55•] and software [37,56] (Figure 3f). Templates may be formed from averaging artifacts [37,48,53,54,55•,56–58] or fitting artifacts to a predefined function type [9,53,59]. These subtraction techniques suffer from varying artifact morphology resulting from undersampling the artifact shape and misalignment of stimulation and sample timing [49•,57]. To improve template accuracy, more complex methods resample and shift the artifact waveforms and templates [57,58]. Similarly, adaptive filtering estimates the artifact by filtering the stimulation pulse [38•] or the artifact recorded on a neighboring channel [60], then subtracts it while filter coefficients are adapted. These subtraction methods can be implemented with low latency, but require artifact detection, template building and on-board memory for template storage. Templates must be updated often to track any changes to artifact shape or stimulus waveform, otherwise signal distortion may occur. Often estimated templates take time to converge, resulting in varying levels of cancellation over time.

Component decomposition methods separate ensembles of recorded channels into artifact and non-artifact components and reconstruct a clean neural signal with only the non-artifact components (Figure 3g). Ensemble empirical mode decomposition [61,62] and independent component analysis [61,63] are common approaches to blindly separating artifacts from neural source. While these methods offer great accuracy in reconstruction, they also involve the most intensive computation, requiring iterative processing steps. Therefore, to our knowledge, they have to date not been implemented for online use.

Front-end and back-end co-design

We have seen that preventative or front-end methods alone are not sufficient for full cancellation of stimulation artifacts. At the same time, adequate artifact prevention and front-end mitigation methods are required to enable back-end cancellation of sampled artifacts. For example, since subtractive algorithms require linearity of superimposed neural and artifact signals, they must be paired with high dynamic range front-ends to prevent signal loss. Therefore, back-end signal processing and resilient front-ends must be co-designed in closed-loop neuromodulation systems for sufficient artifact cancellation.

Two recently designed systems demonstrate this symbiotic combination of artifact cancellation methods. Culaclii *et al*. [37] demonstrate a system that implements template subtraction in two stages separated between the front-end and back-end. Front-end subtraction keeps the recorded signal within the linear range of the amplifiers without requiring gain reduction, and back-end subtraction cancels any remaining artifact. A full system for closed-loop neuromodulation developed by Zhou *et al*. [49•] incorporates the recording and stimulation circuits presented by Johnson *et al*. [19••] and on-board processing for back-end artifact cancellation. The stimulator utilizes preventative charge-balancing techniques, while the front-end also provides a high dynamic range and rapid recovery from artifacts that permits the use of linear interpolation for back-end cancellation, losing only one sample of information in the process. While high dynamic range is not strictly required, it aids the recording front-end to have rapid recovery from the artifact. To our knowledge, this work was the first demonstration of system-wide, on-line, hardware-based artifact cancellation *in vivo*.

Conclusions

Closed-loop neuromodulation holds the promise of transforming disease treatment to be performed in an intelligent, patient-specific, and on-demand manner using devices that learn neurological biomarkers and

Table 1

Comparison of techniques for artifact prevention and mitigation

Methods	Variants	Toward closed-loop
Prevention		
Stimulation pulse charge-balance	Voltage offset correction [16]	Improving charge balance reduces artifact size and duration, relaxing requirements on signal acquisition chain
	Current copying [17,18]	
	Current source reuse [19••,20,21]	
Stimulation waveform design	Tri-phasic stimulation [22]	Compensates for artifact-inducing properties of stimulator, neural tissue and recording circuitry
	Zero-forcing equalization of waveform [23]	
Electrode and reference configuration	Symmetric stim and sense electrode geometry [24••]	Keeps artifact common-mode, which can be tracked by the supply and also cancelled through differential amplification
	Artifact-tracking voltage supply [25]	
Front-end techniques		
Saturation prevention	High Dynamic Range [19••,36]	Keeps recorded artifacts linear, improving the performance of back-end techniques
	Front-end subtraction [32,37,38•,39]	
	Electrode disconnection [1,40–43]	
Rapid recovery	Amplifier charge reset [19••,44]	Recovers from saturation quickly, reduces data loss, and lowers requirements on front-end dynamic range
	High-pass pole shifting [12•,45,56]	
	Active electrode discharge [12•,13,14]	
Back-end techniques		
Data reconstruction	Sample-and-hold interpolation (offline) [47,48]	Simplest to implement and is effective with relaxed SNR requirements
	Linear interpolation (online) [49•]	
	Linear interpolation (offline) [50•]	
	Gaussian interpolation (offline) [51]	
	Cubic spline interpolation (offline) [52]	
Artifact subtraction	Averaged template subtraction (online) [37,55•,56]	Can theoretically remove artifact without distortion to underlying signal if paired with high-dynamic-range front-end
	Averaged template subtraction (offline) [48,53,54]	
	Averaged template resampling and subtraction (offline) [57,58]	
	Function fitting template subtraction (offline) [9,53,59]	
	Adaptive filter (online) [38•]	
Component decomposition	Ensemble empirical mode decomposition (offline) [61,62]	Can remove stimulation artifact while providing other information and removing other types of artifact
	Independent component analysis (offline) [61,63]	

automatically adapt stimulation for optimized therapies. To enable this vision, future devices will have hundreds to thousands (or more) of recording and stimulation channels with embedded signal processing and intelligence. There are numerous challenges in the realization of such devices, and here we have reviewed the state-of-the-art for addressing one key challenge: the ability to perform recording, stimulation, and computation simultaneously and unhindered by stimulation artifacts.

We have presented various artifact mitigation techniques at different points in the stimulation and signal path. Table 1 summarizes these techniques and discusses their key contributions for integration into a closed-loop neuromodulation system. An optimized system must combine preventative, front-end, and back-end techniques, which, in combination, we believe are key to obtaining the best results in recording the full underlying neural signal during stimulation and thereby enabling true closed-loop neuromodulation.

Current recording front-ends with artifact mitigation have already been demonstrated in high density integrated chips, consuming only a few microwatts and occupying less than 0.2 mm^2 per channel [19••,38•]. Back-end artifact cancellation algorithms have been demonstrated in both custom hardware and on-board software running in real time. Platform devices, combining front-end and back-end methods with algorithmic flexibility and reprogrammability, have already been miniaturized to weigh under 18 g with battery lives of over 11 hours [49•], and monolithic integration of these components would result in extremely low power microsystems for improved implant safety and device lifetime. Still, scaling to hundreds or thousands of channels remains a challenge, since conventional front-ends that have achieved significant scaling often trade off artifact-resilient features for improved area. Further research in this area could yield neural interfaces that will completely prevent stimulation artifacts from occurring in the first place and allow for high-performance recording during stimulation without any loss of information.

Conflict of interest statement
Nothing declared.

Acknowledgements

References and recommended reading

Papers of particular interest, published within the period of review, have been highlighted as:

- • of special interest
- •• of outstanding interest

1. Cheng C-H, Tsai P-Y, Yang T-Y, Cheng W-H, Yen T-Y, Luo Z, Qian X-H, Chen Z-X, Lin T-H, Chen W-H *et al.*: **A fully integrated closed-loop neuromodulation SoC with wireless power and bi-directional data telemetry for real-time human epileptic seizure control**. *Symposium on VLSI Circuits*. 2017:C44-C45.

2. Kassiri H, Pazhouhandeh R, Soltani N, Tariqus Salam M, Carlen P, Velazquez JLP, Genov R: **All-wireless 64-channel 0.013 mm²/ch closed-loop neurostimulator with rail-to-rail DC offset removal**. *Dig Tech Pap — IEEE Int Solid-State Circuits Conf* 2017, **60**:452-453.

3. Sun FT, Morrell MJ, Wharen RE: **Responsive cortical stimulation for the treatment of epilepsy**. *Neurotherapeutics* 2008, **5**:68-74.

4. Bronstein JM, Tagliati M, Alterman RL, Lozano AM, Volkmann J, Stefani A, Horak FB, Okun MS, Foote KD, Krack P *et al.*: **Deep brain stimulation for parkinson disease**. *Arch Neurol* 2011, **68**:165.

5. Benabid AL, Chabardes S, Mitrofanis J, Pollak P: **Deep brain stimulation of the subthalamic nucleus for the treatment of Parkinson's disease**. *Lancet Neurol* 2009, **8**:67-81.

6. Khanna P, Stanslaski S, Xiao Y, Ahrens T, Bourget D, Swann N, Starr P, Carmena JM, Denison T: **Enabling closed-loop neurostimulation research with downloadable firmware upgrades**. *2015 IEEE Biomedical Circuits and Systems Conference*. 2015.

7. Rhew HG, Jeong J, Fredenburg JA, Dodani S, Patil PG, Flynn MP: **A fully self-contained logarithmic closed-loop deep brain stimulation SoC with wireless telemetry and wireless power management**. *IEEE J Solid-State Circuits* 2014, **49**:2213-2227.

8. Rosin B, Slovik M, Mitelman R, Rivlin-Etzion M, Haber SN, Israel Z, Vaadia E, Bergman H: **Closed-loop deep brain stimulation is superior in ameliorating parkinsonism**. *Neuron* 2011, **72**:370-384.

9. Wagenaar DA, Potter SM: **Real-time multi-channel stimulus artifact suppression by local curve fitting**. *J Neurosci Methods* 2002, **120**:113-120.

10. Merrill DR, Bikson M, Jefferys JGR: **Electrical stimulation of excitable tissue: design of efficacious and safe protocols**. *J Neurosci Methods* 2005, **141**:171-198.

11. Wang C, Brunton E, Haghgooie S, Cassells K, Lowery A, Rajan R: **Characteristics of electrode impedance and stimulation efficacy of a chronic cortical implant using novel annulus electrodes in rat motor cortex**. *J Neural Eng* 2013, **10**:46010.

12. Brown EA, Ross JD, Blum RA, Nam Y, Wheeler BC, DeWeerth SP:
• **Stimulus artifact elimination in a multi-electrode system**. *IEEE Trans Biomed Circuits Syst* 2008, **2**:10-21.
This paper describes a front-end neural amplifier with active electrode discharge circuitry for rapid recovery from artifacts. Following stimulus, a feedback amplifier drives electrode voltage back to an averaged DC voltage stored from before the stimulation pulse. This work, along with earlier publications [13,14], highlighted the importance of understanding and modeling electrode behavior to aid in amplifier design.

13. Blum RA, Member S, Ross JD, Member S, Brown EA, Member S, Deweerth SP, Member S: **An integrated system for simultaneous, multichannel neuronal stimulation and recording**. *IEEE Trans Circuits Syst I Regul Pap* 2007, **54**:2608-2618.

14. Blum R, Ross J, Das S, Brown E, Deweerth S: **Models of stimulation artifacts applied to integrated circuit design**. In *Proceedings of the 26th Annual International Conference of the IEEE EMBS*. 2004:4075-4078.

15. Wagenaar DA, Pine J, Potter SM: **Effective parameters for stimulation of dissociated cultures using multi-electrode arrays**. *J Neurosci Methods* 2004, **138**:27-37.

16. Noorsal E, Sooksood K, Xu H, Hornig R, Becker J, Ortmanns M: **A neural stimulator frontend with high-voltage compliance and programmable pulse shape for epiretinal implants**. *IEEE J Solid-State Circuits* 2012, **47**:244-256.

17. Greenwald E, Chen C, Thakor N, Maier C, Cauwenberghs G: **A CMOS neurostimulator with on-chip DAC calibration and charge balancing**. *2013 IEEE Biomedical Circuits and Systems Conference (BioCAS)*; IEEE: 2013:89-92.

18. Sit J-J, Sarpeshkar R: **A low-power blocking-capacitor-free charge-balanced electrode-stimulator chip with less than 6 nA DC error for 1-mA full-scale stimulation**. *IEEE Trans Biomed Circuits Syst* 2007, **1**:172-183.

19. Johnson BC, Gambini S, Izyumin I, Moin A, Zhou A, Alexandrov G,
•• Santacruz SR, Rabaey JM, Carmena JM, Muller R: **An implantable 700W 64-channel neuromodulation IC for simultaneous recording and stimulation with rapid artifact recovery**. *Symposium on VLSI Circuits*; IEEE: 2017:C48-C49.
This paper describes a VLSI neuromodulator combining artifact prevention and mitigation techniques. Four current source reuse stimulators allow for precisely charge-balanced stimulation pulses. 64 mixed-signal front-ends with large input ranges and memoryless sampling provide rapid recovery from artifacts. Recorded artifacts are short in duration and artifact timing is appended to the digital samples, allowing for easy system integration.

20. Pepin E, Uehlin J, Micheletti D, Perlmutter SI, Rudell JC: **A high-voltage compliant, electrode-invariant neural stimulator front-end in 65 nm bulk-CMOS**. *ESSCIRC Conference 2016: 42nd European Solid-State Circuits Conference*; IEEE: 2016:229-232.

21. Shulyzki R, Abdelhalim K, Bagheri A, Salam MT, Florez CM, Velazquez JLP, Carlen PL, Genov R: **320-Channel active probe for high-resolution neuromonitoring and responsive neurostimulation**. *IEEE Trans Biomed Circuits Syst* 2015, **9**:34-49.

22. Bahmer A, Peter O, Baumann U: **Recording and analysis of electrically evoked compound action potentials (ECAPs) with MED-EL cochlear implants and different artifact reduction strategies in Matlab**. *J Neurosci Methods* 2010, **191**:66-74.

23. Chu P, Muller R, Koralek A, Carmena JM, Rabaey JM, Gambini S: **Equalization for intracortical microstimulation artifact reduction**. In *Proceedings of the Annual International Conference of the IEEE Engineering in Medicine and Biology Society, EMBS*. 2013:245-248.

24. Stanslaski S, Afshar P, Cong P, Giftakis J, Stypulkowski P,
•• Carlson D, Linde D, Ullestad D, Avestruz AT, Denison T: **Design and validation of a fully implantable, chronic, closed-loop neuromodulation device with concurrent sensing and stimulation**. *IEEE Trans Neural Syst Rehabil Eng* 2012, **20**:410-421.
This paper presents several system-level methods and experiment design considerations to prevent and mitigate the effect of stimulation artifacts. Most notably, stimulation and recording electrode configuration and geometry are optimized to present artifact as a common-mode signal that can be cancelled by differential front-ends. Careful selection of stimulation parameters and sampling frequency is also discussed. The paper validates these methods in an implantable system for closed-loop neuromodulation.

25. Peterson EJ, Dinsmoor DA, Tyler DJ, Denison TJ: **Stimulation artifact rejection in closed-loop, distributed neural interfaces**. *2016 European Solid-State Circuits Conference*. 2016:233-236.

26. Muller R, Le H-P, Li W, Ledochowitsch P, Gambini S, Bjorninen T, Koralek A, Carmena JM, Maharbiz MM, Alon E *et al.*: **A Minimally invasive 64-channel wireless μECoG implant**. *IEEE J Solid-State Circuits* 2015, **50**:344-359.

27. Harrison RR, Watkins PT, Kier RJ, Lovejoy RO, Black DJ, Greger B, Solzbacher F: **A low-power integrated circuit for a wireless**

100-electrode neural recording system. *IEEE J Solid-State Circuits* 2007, **42**:123-133.

28. Muller R, Gambini S, Rabaey JM: **A 0.013 mm², 5 µW, DC-coupled neural signal acquisition IC with 0.5 V supply**. *IEEE J Solid-State Circuits* 2012, **47**:232-243.

29. Fan Zhang, Holleman J, Otis BP: **Design of ultra-low power biopotential amplifiers for biosignal acquisition applications**. *IEEE Trans Biomed Circuits Syst* 2012, **6**:344-355.

30. Johnson B, Molnar A: **An orthogonal current-reuse amplifier for multi-channel sensing**. *IEEE J Solid-State Circuits* 2013, **48**:1487-1496.

31. Harrison RR, Charles C: **A low-power low-noise cmos for amplifier neural recording applications**. *IEEE J Solid-State Circuits* 2003, **38**:958-965.

32. Smith WA, Uehlin JP, Perlmutter SI, Rudell JC, Sathe VS: **A scalable, highly-multiplexed delta-encoded digital feedback ecog recording amplifier with common and differential-mode artifact suppression**. *Symposium on VLSI Circuits*. 2017:C172-C173.

33. Lopez CM, Mitra S, Putzeys J, Raducanu B, Ballini M, Andrei A, Severi S, Welkenhuysen M, Van Hoof C, Musa S *et al.*: **22.7 A 966-electrode neural probe with 384 configurable channels in 0.13 µm SOI CMOS**. *2016 IEEE International Solid-State Circuits Conference (ISSCC)*; IEEE: 2016:392-393.

34. Johnson B, Peace ST, Cleland TA, Molnar A: **A 50 µm pitch, 1120-channel, 20 kHz frame rate microelectrode array for slice recording**. *2013 IEEE Biomedical Circuits and Systems Conference (BioCAS)*; IEEE: 2013:109-112.

35. Park S-Y, Cho J, Yoon E: **3.37 µW/Ch modular scalable neural recording system with embedded lossless compression for dynamic power reduction**. *2017 Symposium on VLSI Circuits*; IEEE: 2017:C168-C169.

36. Rolston JD, Gross RE, Potter SM: **A low-cost multielectrode system for data acquisition enabling real-time closed-loop processing with rapid recovery from stimulation artifacts**. *Front Neuroeng* 2009, **2**:12.

37. Culaclii S, Kim B, Lo YK, Liu W: **A hybrid hardware and software approach for cancelling stimulus artifacts during same-electrode neural stimulation and recording**. In *Proceedings of the Annual International Conference of the IEEE Engineering in Medicine and Biology Society, EMBS*. 2016:6190-6193.

38. Mendrela AE, Cho J, Fredenburg JA, Nagaraj V, Netoff TI,
• Flynn MP, Yoon E: **A bidirectional neural interface circuit with active stimulation artifact cancellation and cross-channel common-mode noise suppression**. *IEEE J Solid-State Circuits* 2016, **51**:955-965.
This paper describes a mixed-signal approach for artifact cancellation. The stimulation signal is digitally filtered through a least mean squares adaptive filter, then converted into an analog signal and subtracted from the front-end amplifier. This subtraction eases the dynamic range requirements for the amplifier and does not require knowledge of stimulation parameters. A common average referencing scheme is also implemented to reduce the effects of noise common to all channels.

39. Nag S, Sikdar SK, Thakor NV, Rao VR, Sharma D: **Sensing of stimulus artifact suppressed signals from electrode interfaces**. *IEEE Sens J* 2015, **15**:3734-3742.

40. Hottowy P, Skoczeń A, Gunning DE, Kachiguine S, Mathieson K, Sher A, Wia?cek P, Litke AM, Da?browski W: **Properties and application of a multichannel integrated circuit for low-artifact, patterned electrical stimulation of neural tissue**. *J Neural Eng* 2012, **9**:66005.

41. Venkatraman S, Elkabany K, Long JD, Yao Y, Carmena JM: **A system for neural recording and closed-loop intracortical microstimulation in awake rodents**. *IEEE Trans Biomed Eng* 2009, **56**:15-22.

42. DeMichele GA, Troyk PR: **Stimulus-resistant neural recording amplifier**. In *Proceedings of the 25th Annual Conference of the IEEE EMBS*. 2003:3329-3332.

43. Jimbo Y, Kasai N, Torimitsu K, Tateno T, Robinson HPC: **A system for MEA-based multisite stimulation**. *IEEE Trans Biomed Eng* 2003, **50**:241-248.

44. Heer F, Hafizovic S, Ugniwenko T, Frey U, Franks W, Perriard E, Perriard JC, Blau A, Ziegler C, Hierlemann A: **Single-chip microelectronic system to interface with living cells**. *Biosens Bioelectron* 2007, **22**:2546-2553.

45. Viswam V, Chen Y, Shadmani A, Dragas J, Bounik R, Milos R, Muller J, Hierlemann A: **2048 action potential recording channels with 2.4 µVrms noise and stimulation artifact suppression**. *2016 IEEE Biomed Circuits Syst Conf*. 2016 http://dx.doi.org/10.1109/BioCAS.2016.7833750.

46. Olsson RH, Buhl DL, Sirota AM, Buzsaki G, Wise KD: **Band-tunable and multiplexed integrated circuits for simultaneous recording and stimulation with microelectrode arrays**. *IEEE Trans Biomed Eng* 2005, **52**:1303-1311.

47. Hartmann C, Dosen S, Amsuess S, Farina D: **Closed-loop control of myoelectric prostheses with electrotactile feedback: influence of stimulation artifact and blanking**. *IEEE Trans Neural Syst Rehabil Eng* 2015, **23**:807-816.

48. Montgomery EB, Gale JT, Huang H: **Methods for isolating extracellular action potentials and removing stimulus artifacts from microelectrode recordings of neurons requiring minimal operator intervention**. *J Neurosci Methods* 2005, **144**:107-125.

49. Zhou A, Santacruz SR, Johnson BC, Alexandrov G, Moin A,
• Burghardt FL, Rabaey JM, Carmena JM, Muller R: *WAND: A 128-Channel, Closed-loop Wireless Artifact-free Neuromodulation Device*. 2017. ar***Xiv:1708.00556.
This paper describes the *in vivo* application of a closed-loop neuromodulation device for delivering stimulation while simultaneously recording LFP. Custom front-end stimulation and recording circuits [19] are integrated with back-end digital processing to completely removed artifacts. Linear interpolation is shown to allow for accurate recovery of the LFP power spectral density. Beta-band modulation is used to control stimulation and is accurately recovered even during stimulation pulse trains.

50. Heffer LF, Fallon JB: **A novel stimulus artifact removal
• technique for high-rate electrical stimulation**. *J Neurosci Methods* 2008, **170**:277-284.
This paper describes a method of linear interpolation for removing artifacts. Although presented as an offline, post-processing method, the authors recognized the need for a computationally efficient algorithm that could be implemented in hardware for real-time operation.

51. Hoffmann U, Cho W, Ramos-Murguialday A, Keller T: **Detection and removal of stimulation artifacts in electroencephalogram recordings**. *Proc Annu Int Conf IEEE Eng Med Biol Soc EMBS*. 2011 http://dx.doi.org/10.1109/IEMBS.2011.6091809.

52. Waddell C, Pratt JA, Porr B, Ewing S: **Deep brain stimulation artifact removal through under-sampling and cubic-spline interpolation**. *2009 2nd International Congress on Image and Signal Processing*; IEEE: 2009:1-5.

53. Erez Y, Tischler H, Moran A, Bar-Gad I: **Generalized framework for stimulus artifact removal**. *J Neurosci Methods* 2010, **191**:45-59.

54. Hashimoto T, Elder CM, Vitek JL: **A template subtraction method for stimulus artifact removal in high-frequency deep brain stimulation**. *J Neurosci Methods* 2002, **113**:181-186.

55. Limnuson K, Lu H, Chiel HJ, Mohseni P: **Real-time stimulus
• artifact rejection via template subtraction**. *IEEE Trans Biomed Circuits Syst* 2014, **8**:391-400.
This paper describes a hardware-implemented filter for online back-end template subtraction. Templates are formed by averaging artifacts. The paper also presents methods for optimizing filter performance, including optimal initialization of filter memory and implementation with fixed-point computation.

56. Wichmann T, Devergnas A: **A novel device to suppress electrical stimulus artifacts in electrophysiological experiments**. *J Neurosci Methods* 2011, **201**:1-8.

57. Qian X, Chen Y, Feng Y, Ma B, Hao H, Li L: **A method for removal of deep brain stimulation artifact from local field potentials**. *IEEE Trans Neural Syst Rehabil Eng* 2016, **PP**.

58. Sun L, Hinrichs H: **Moving average template subtraction to remove stimulation artefacts in EEGs and LFPs recorded during deep brain stimulation**. *J Neurosci Methods* 2016, **266**:126-136.

59. Trebaul L, Rudrauf D, Job AS, Mălîia MD, Popa I, Barborica A, Minotti L, Mîndruţă I, Kahane P, David O: **Stimulation artifact correction method for estimation of early cortico-cortical evoked potentials**. *J Neurosci Methods* 2016, **264**:94-102.

60. Basir-kazeruni S, Vlaski S, Salami H, Sayed AH, Markovi D: **A blind adaptive stimulation artifact rejection (ASAR) engine for closed-loop implantable neuromodulation systems**. In *Proceedings of the 8th International IEEE EMBS Conference on Neural Engineering*. 2017:186-189.

61. Zeng K, Chen D, Ouyang G, Wang L, Liu X, Li X: **An EEMD-ICA approach to enhancing artifact rejection for noisy multivariate neural data**. *IEEE Trans Neural Syst Rehabil Eng* 2016, **24**:630-638.

62. Al-ani T, Cazettes F, Palfi S, Lefaucheur JP: **Automatic removal of high-amplitude stimulus artefact from neuronal signal recorded in the subthalamic nucleus**. *J Neurosci Methods* 2011, **198**:135-146.

63. Lu Y, Cao P, Sun J, Wang J, Li L, Ren Q, Chen Y, Chai X: **Using independent component analysis to remove artifacts in visual cortex responses elicited by electrical stimulation of the optic nerve**. *J Neural Eng* 2012, **9**:2600.